

An acoustic micrometer and its application to layer thickness measurements

著者	櫛引 淳一
journal or publication title	IEEE Ultrasonics, Ferroelectrics and Frequency Control
volume	36
number	3
page range	326-331
year	1989
URL	http://hdl.handle.net/10097/46472

doi: 10.1109/58.19171

An Acoustic Micrometer and Its Application to Layer Thickness Measurements

YUSUKE TSUKAHARA, MEMBER, IEEE, NORITAKA NAKASO, JUN-ICHI KUSHIBIKI, MEMBER, IEEE,
AND NORIYOSHI CHUBACHI, MEMBER, IEEE

Abstract—When an ultrasonic wave propagating to a medium such as water is incident upon a layered surface, the power spectrum of the reflected ultrasonic wave exhibits a dip at a specific frequency that corresponds to the excitation of pseudo-Sezawa waves on the surface. The phenomenon has been successfully incorporated in an acoustic micrometer for layer thickness measurements. The paper describes the principle and system of the acoustic micrometer. Its basic performance, in respect to the stability, accuracy, spatial resolution and temperature dependence, has also been discussed. Gold layers electroplated on substrates of 42 percent Ni-Fe alloy were taken as test specimens in the present study. The measurable range of the thickness for gold layers covered from 1–20 μm by using a frequency range of 10–200 MHz. The stability and accuracy have been achieved to within ± 0.2 percent and ± 1 percent, respectively.

I. INTRODUCTION

MEASUREMENTS of the film thickness in layered structures have become an important technology in the micro electronic industry. For the thickness measurement, various nondestructive methods are known so far such as X-ray fluorescence method [1], ultrasonic interferometry [2], $V(z)$ curve analysis in acoustic microscopy [3], [4], and methods using surface profilers [5], [6]. These methods are, however, not appropriate for the measurements in the production line. The X-ray fluorescence method is widely employed for the layer thickness measurement of electronic components, such as lead frames of LSI's and printed circuit boards. This method requires longer than ten seconds for measurements, so that it is not suitably applied to the measurements in the production line. In ultrasonic interferometry, sufficient sensitivity cannot be obtained for such layered structures as lead frames of large-scale integrations (LSIs), because the combination of acoustic impedances of the layer and substrate in such cases does not permit a sufficient magnitude of resonance [2]. The $V(z)$ methods can be applied with a very high accuracy [4], but it requires precise movements of an acoustic lens, which is difficult to realize when measurements are made in the production line. The surface profilers cannot be used for layer thickness measure-

ments if the entire surface of a substrate is covered with an opaque layer.

In previous papers [7], [8], we have developed a new method of the layer thickness measurement, which can be stably used in the production line of microelectronic products. The method was successfully implemented into an acoustic micrometer.

The purpose of the present paper is to describe the acoustic micrometer and to examine factors that dominantly influence its basic performance. The principle of the measurement is first described. The construction of the acoustic micrometer and its function are explained. The basic performance of the acoustic micrometer, including the stability, accuracy and spatial resolution, is then discussed, because they are important factors for industrial applications. The temperature dependence of measurements is also discussed. When the acoustic micrometer is introduced in the production line, a large amount of mechanical allowance in the positioning of a sensor is desirable to obtain stable measurements. Therefore, the effect of the sensor positioning on measurements is finally discussed.

II. PRINCIPLE OF MEASUREMENT

We suppose that a semiinfinite substrate occupies a lower half space, and a layer with the thickness d covers the surface of the substrate. It is well known that a number of modes of surface waves can be propagated along the surface, if the transverse sound velocity in the layer is less than that in the substrate [9]. The fundamental mode is of a Rayleigh wave, and the second mode is of a Sezawa wave [10]. Then, we suppose that the upper half space is filled with fluid, typically water, and an ultrasonic plane wave is incident onto the layered surface with an incident angle θ as shown in Fig. 1. Dispersion curves of phase velocities for the first two modes, which can be excited on the surface by the incident wave, are shown in Fig. 2. The layer and substrate are of gold and 42-alloy (42 percent Ni-Fe alloy), respectively, which are familiar materials in the micro electronic industry. In the figure, the wave number k is normalized to a dimensionless variable $kd/2\pi$. The Sezawa wave has a cut-off wave number, at which the phase velocity is equal to the transverse sound velocity in the substrate. The Sezawa wave is usually defined for the wave number greater than the cut-off wave

Manuscript received August 1, 1988; revised and accepted October 25, 1988.

Y. Tsukahara and N. Nakaso are with Technical Research Institute, Toppan Printing Co., Ltd., Sugito-machi, Saitama-prefecture 345, Japan.

J. Kushibiki and N. Chubachi are with Department of Electrical Engineering, Faculty of Engineering, Tohoku University, Sendai 980, Japan.

IEEE Log Number 8926471.

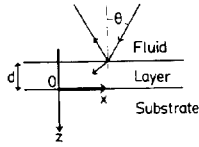


Fig. 1. Coordinate system for layered half space.

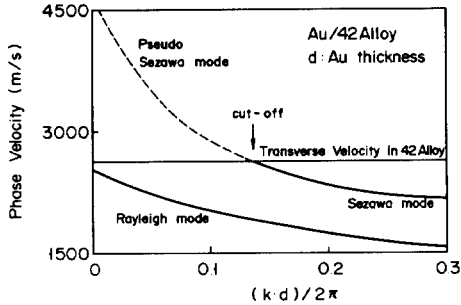


Fig. 2. Dispersion curves of surface waves excited on layered half space, loaded with water. Layer: gold, substrate: 42-alloy.

number, as indicated with a solid line in Fig. 2. A dashed line in the figure is for a pseudo-Sezawa wave, which is a kind of leaky surface wave. The pseudo-Sezawa wave cannot propagate along the surface without attenuation, but radiates its energy into the substrate and decreases exponentially [11].

If the frequency and incident angle of the incident wave satisfy the condition of excitation of the pseudo-Sezawa wave, then some portion of the incident energy transmits into the substrate, and therefore, the energy of the reflected wave is reduced. This mechanism is illustrated in Fig. 3. Fig. 3(a) schematically shows the wave propagation when the pseudo-Sezawa wave is excited, while Fig. 3(b) shows the wave propagation when the Sezawa or Rayleigh wave is excited.

This phenomenon can be theoretically obtained as dips in the angular and frequency dependence of a reflection coefficient $R(fd, \theta)$ for the layered surface [7]. The fd value is the product of frequency f and layer thickness d . The calculation of $R(fd, \theta)$ was made according to Chimenti *et al.* [12], in which attenuation of ultrasonic waves in solids was neglected for the sake of simplicity. The functional dependence of the reflection coefficient $R(fd, \theta)$ on the incident angle θ and fd value is shown in Fig. 4. The absolute value of $R(fd, \theta)$ is plotted as to be zero on top and unity at bottom, therefore, the deepest dip is seen as a steep peak where $fd = 0.275$ km/sec and $\theta = 31^\circ$. Because no loss was assumed in the calculation, the existence of the dips in the reflection coefficient means that corresponding amounts of energy transmit into the substrate. From the location of the dips in the $fd - \theta$ plane, phase velocity V and wave number k of the pseudo-Sezawa wave can be obtained by using Snell's law and the definition of the phase velocity as shown in (1) and (2)

$$V = V_w / \sin \theta, \quad (1)$$

$$kd/2\pi = fd/V, \quad (2)$$

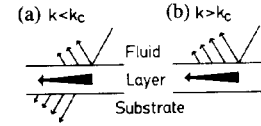
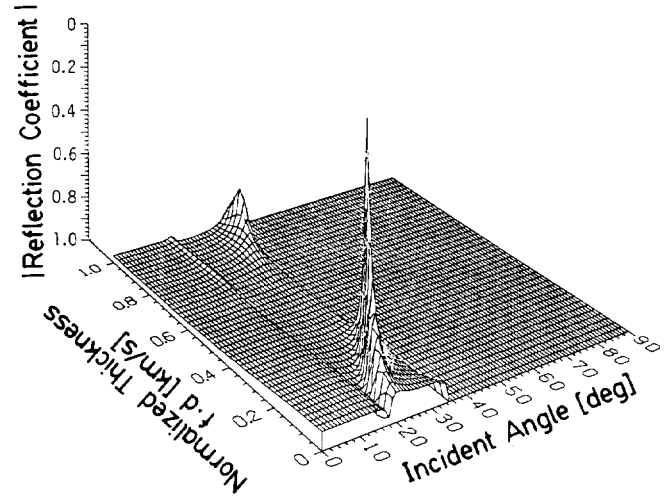


Fig. 3. Schematic drawing of wave propagation on layered surface, (a) when pseudo-Sezawa wave is excited; (b) when Sezawa or Rayleigh wave is excited.


 Fig. 4. Reflection coefficient calculated as function of incident angle θ and fd value for the layered structures of gold layer on 42-alloy substrate.

where V_w is the sound velocity in water. The deepest dip in Fig. 4 corresponds to the pseudo-Sezawa wave excited with a wave number slightly less than the cut off wave number. In this situation the majority of the incident energy transmits into the substrate. This condition is practically realized by setting the incident angle at an appropriate value θ_0 , as shown in (3).

$$\sin \theta_0 = V_w / V_c, \quad (3)$$

where V_c is the phase velocity of the pseudo-Sezawa wave at the cut off wave number. The appropriate incident angle θ_0 is, from Fig. 4, 31° or less for a 42-alloy substrate with a gold layer.

Once the incident angle and materials of both layer and substrate are determined, then the fd value is uniquely determined to a specific value, $(fd)_c$. Therefore, the layer thickness d can be estimated by measuring the dip frequency f and by calculating $d = (fd)_c / f$.

III. INSTRUMENT

A block diagram of an acoustic micrometer is shown in Fig. 5. An ultrasonic sensor consisted of a pair of transducer rods. An electrical impulse generated by a pulse generator was applied to a piezoelectric transducer. Acoustic waves reflected at the surface of a specimen were received by the other transducer, and the electrical output signal was fed into an amplifier. The first pulse in the reflected wave was extracted by using a gate circuit. The power spectrum of the extracted signal was obtained by a spectrum analyzer. A controller detected a dip in the power spectrum and converted the dip frequency into the

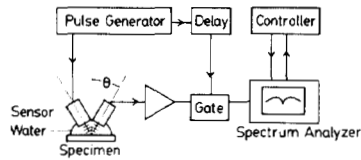


Fig. 5. Block diagram of acoustic micrometer.

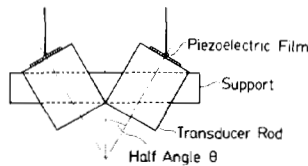


Fig. 6. Schematic drawing of ultrasonic sensor.

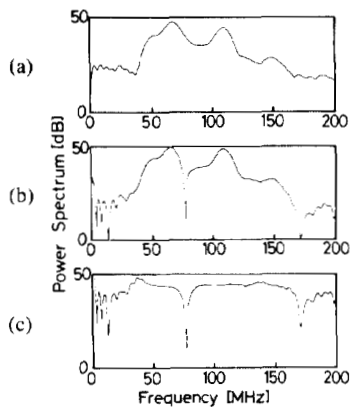


Fig. 7. Normalization of power spectra. (a) Spectrum for 42-alloy specimen with no layer. (b) Spectrum for specimen with 3.1 μm gold layer. (c) Normalized spectrum ((a)-(b)).

layer thickness. Furthermore, the controller calibrated the temperature dependence of the measured values because it could affect the accuracy of the measurements.

The voltage of the applied impulse was 200 v over a duration of 5 ns. The ultrasonic sensor is schematically drawn in Fig. 6. The material of the piezoelectric transducer was ZnO film, which was sputtered on one side of the transducer rod made of fused quartz. The diameter and the length of the transducer rod were 8 mm and 10 mm, respectively. The effective frequency range of the transducer was 30–150 MHz. The half angle, denoted by θ in Fig. 6, was set at specific values between 27° and 31° , at which a deep dip in the power spectrum could be obtained for a 42-alloy substrate with a gold layer.

The operation of the acoustic micrometer is as follows. Prior to the measurement, the frequency response of the measurement system should be estimated by measuring the power spectrum of waves reflected by the substrate with no layer on it (See Fig. 7(a)). This spectrum should be stored as a reference spectrum. Only the effect due to the layer deposition, Fig. 7(c), can be obtained by dividing the power spectrum for a layered substrate, Fig. 7(b), with the reference spectrum, in order to cancel the effect of the frequency response of the measurement system. Finally, the layer thickness can be obtained from the dip frequency in the power spectrum, Fig. 7(c), as explained in the previous section.

IV. EXPERIMENTS ON PERFORMANCE

In order to attain the performance of the acoustic micrometer required for the thickness measurement of layered products in the production line, the following problems were experimentally investigated: a) temperature dependence; b) stability and accuracy; c) spatial resolution; and d) effect of sensor-positioning on measurements.

For all experiments, substrates of 42-alloy with gold layers were employed as test specimens.

A. Temperature Dependence

Let us k and f be the wave number and frequency of the pseudo-Sezawa wave, respectively, and V_w and V be the sound velocity in water and the phase velocity of the pseudo-Sezawa wave, respectively. The incident angle is θ . By rearranging (2), the dip frequency f is related to V and k as

$$f = Vk/2\pi. \quad (4)$$

Since the wave number k is dependent on the phase velocity V through the dispersion relation as graphically shown in Fig. 1, the frequency f can be regarded as a function of V ,

$$f(V) = Vk(V)/2\pi. \quad (5)$$

As evident from (1), the phase velocity V depends on V_w , which changes significantly with temperature, therefore, the dip frequency f also depends on temperature through (5). Although such quantities as sound velocities in the substrate and layer materials also depend on temperature, the amount of the change in them is much less than that in V_w . Thus, the dip frequency depends on temperature, mainly because the sound velocity in water changes with temperature.

In order to obtain calibration curves of the dip frequency as a function of temperature, the following experiments were made. Two specimens were used, the layer thickness of which was 5.2 μm and 7.2 μm , respectively, measured by the conventional X-ray fluorescence method [1]. The thickness of substrates was 2 mm. The incident angle was 27.4° . The frequency resolution of the spectral analysis was chosen at 0.125 MHz, according to a reason to be discussed in section B. Temperature was changed from 10°C to 40°C . The rate of change was maintained within $3^\circ\text{C}/\text{hour}$ to keep a homogeneity of temperature of water and specimens. The dependence of the dip frequency on temperature is plotted in Fig. 8 for the 7.2 μm specimen. Dotted lines are measured data, while the solid line is a quadratic curve, fitted to the data by the method of least squares. The measured data are well represented by the least-square-curve, therefore, it is obvious that the calibration of temperature dependence can be accomplished by referring to such calibration curves.

B. Stability and Accuracy

As seen from Fig. 8, dip frequencies were stably measured within the minimum resolution of the frequency analysis (0.125 MHz). Therefore, it was estimated that

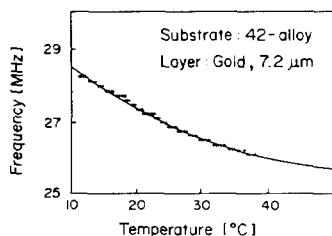


Fig. 8. Dependence of dip frequencies on temperature. Incident angle— 27.4° ; frequency resolution— 0.125 MHz. Solid line is quadratic curve least-squares-fitted.

the stability of the measurement was achieved at least to within ± 0.2 percent. In general, the spectrum analyzer sweeps in the slower rate for higher resolution, and furthermore, such noise reduction techniques as averaging or maximum holding are required to achieve precise measurements. Therefore, the minimum resolution and measurement time are traded off for each other. In the present study, we have chosen the resolution of 0.125 MHz and measurement time of one second, which were suitable for measurements in the production line of electronic components.

Experiments were made on two specimens with different layer thicknesses, $5.2 \mu\text{m}$ and $7.2 \mu\text{m}$, and measured data are plotted in Fig. 9. In the figure, dip frequencies were normalized to fd values by multiplication with the thickness d . The fd values for the two specimens with different layer thickness exhibit a discrepancy of ± 1 percent, which bounds the upper limit of the absolute accuracy in this case. It was, however, difficult to estimate the absolute accuracy, more precisely in this experiment. The accuracy of the X-ray fluorescence method, which was used to obtain the reference values of the layer thickness, was limited to within a few percent.

C. Spatial Resolution

When the measurement is made on layered products in the production line, it is usually sufficient only to measure the average layer thickness over a part of the layered surface. However, it sometimes is required to measure the spatial distribution of the layer thickness. The spatial resolution of the measurement was, therefore, investigated through modification of the ultrasonic sensor.

A mask with an aperture hole was attached on the transducer rod to obtain a narrow beam as shown in Fig. 10. The material of the mask was silicon rubber. In this experiment, we employed a test specimen with its surface partially electroplated with gold of $4.5 \text{ mm} \times 5 \text{ mm}$ in the surface area and $3.1 \mu\text{m}$ in the average thickness. The cross sectional view of the specimen, obtained by a surface profiler [14] is drawn in Fig. 11(b). One dimensional distribution of the layer thickness, measured by using an ultrasonic sensor with an aperture diameter of 0.6 mm , is also plotted in Fig. 11(a). From the observation of measured data at the edges of the layer in Fig. 11, we could estimate that the spatial resolution in this case was about 0.5 mm . When a mask with aperture diameter less than 0.5 mm was used, the power of the ultrasonic beam be-

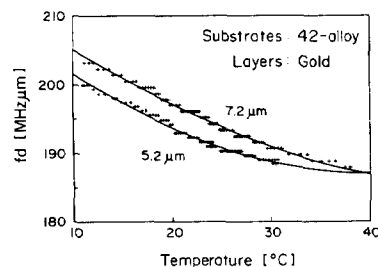


Fig. 9. Dependence of fd values on temperature.

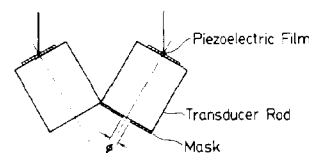


Fig. 10. Illustration of ultrasonic sensor. Mask with aperture is placed on transducer rod.

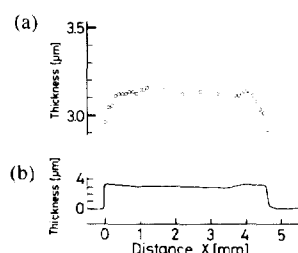


Fig. 11. One-dimensional distribution of layer thickness. (a) Measured with ultrasonic sensor having mask on it. (b) Obtained by surface profiler.

came so weak that an accurate measurement could not be made. Therefore, minimum spatial resolution obtained in this experiment was estimated to be 0.5 mm .

The higher spatial resolution might be possible if an acoustic lens is employed for the transducer rod, a study of which will be treated elsewhere.

D. Sensor-Positioning

Misalignments in set up of a sensor (displacement z along the normal to the surface of a specimen, and inclination ψ around the proper incident angle, as shown in Fig. 12) result in a degradation of the accuracy of thickness measurements. It is desirable to have large allowances in the sensor-positioning for rapid and stable measurements, because the acoustic micrometer has been primarily aimed at applications in the factory environment.

The following experiments were made to estimate the allowances in z and ψ . The layer thickness of a test specimen was $3.1 \mu\text{m}$. Incident angle was 29.7° . Peak to peak voltages of reflected waveforms, V_{pp} , and dip frequencies in spectra were measured while changing the distance between the sensor and specimen. In Fig. 13, relative output power of the receiving transducer, namely $20 \log_{10} V_{pp}$, and dip frequencies in spectra are plotted with \bullet and \circ , respectively, as functions of the displacement z of the sensor. It can be seen from the figure that the dip frequency remained in a region from 71.75 MHz to 72.5 MHz when

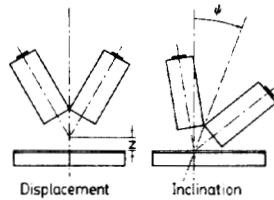


Fig. 12. Illustration showing displacement and inclination of ultrasonic sensor.

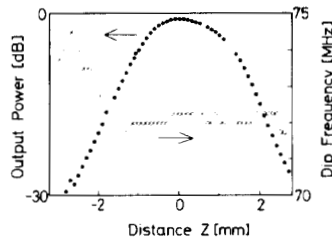


Fig. 13. Dependence of output voltages and dip frequencies on sensor displacement. Layer thickness: $3.1 \mu\text{m}$.

the sensor was displaced along the normal to the surface of the specimen up to ± 2 mm from its focus at $z = 0$. The dip frequency deviated considerably when the sensor was displaced more than ± 2 mm. The allowance in the sensor displacement was thus estimated to be ± 2 mm.

Further experiments were performed in order to assess the allowance in the sensor inclination. Peak to peak voltages of reflected waveforms, V_{pp} , and dip frequencies in spectra were measured as above while changing the sensor inclination, ψ . Relative output power of the receiving transducer, $20 \log_{10} V_{pp}$, and dip frequencies in spectra are plotted with \bullet and \circ , respectively, as functions of the sensor inclination. It can be seen from Fig. 14 that the dip frequency remained virtually unchanged when the sensor inclination was within $\pm 0.2^\circ$. The dip frequency deviated considerably when the inclination exceeded $\pm 0.2^\circ$. Therefore, the allowance in the inclination was estimated to be $\pm 0.2^\circ$.

The experiments in this section have shown that the sensor-positioning should be maintained within the allowances ($|z| < 2$ mm, $|\psi| < 0.2^\circ$) in order to accurately obtain the dip frequency. This can be easily performed by adjusting the sensor-positioning so that the peak voltage of the reflected waveform is maximum.

E. Limitations

In the present method, the measurable range of the thickness is limited by the effective frequency range of the ultrasonic sensor, because the dip frequency is inversely proportional to the layer thickness. At present, it is difficult to measure the layer thickness less than $1 \mu\text{m}$. On the contrary, such layer thickness less than $1 \mu\text{m}$ is accurately measured with an acoustic microscope [13]. The measurement with an acoustic microscope becomes difficult if the layer thickness is large, because multiple modes of surface waves are then excited. Therefore, the two methods can be used complementarily.

An evaluation of the accuracy made in Section IV-B,

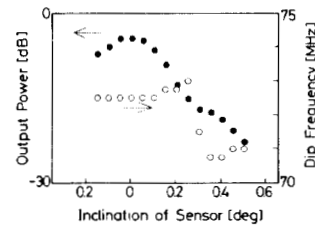


Fig. 14. Dependence of output voltages and dip frequencies on sensor inclination. Layer thickness: $3.1 \mu\text{m}$.

was limited up to one percent because of the limited accuracy of the X-ray fluorescence method. One of other possible sources of limitation in the accuracy might be a dependence of fd values on variations of acoustic properties (density, sound velocity, etc.) for specimens with different layer thickness. And fd values might also depend on adhesion of layers. These sources of limitation in the accuracy, at the same time, suggest a possibility to detect variations of acoustic properties and adhesion of layers. The possibility will be explored elsewhere with regard to the measurement of quality of layers.

V. CONCLUSION

An acoustic micrometer for layer thickness measurement using pseudo-Sezawa waves was developed. The acoustic micrometer was constructed, based on a phenomenon that the pseudo-Sezawa wave was excited on a layered surface by an obliquely incident ultrasonic wave. The performance, which was required for the measurement in the production line, was experimentally investigated by using test specimens consisting of 42-alloy substrates with gold layers. The performance was achieved as follows. Measurable thickness range; $1\text{--}20 \mu\text{m}$, stability; ± 0.2 percent, accuracy; ± 1 percent, minimum spatial resolution; 0.5 mm, measurement time; 1 s.

ACKNOWLEDGMENT

The authors wish to extend their gratitude to Hitoshi Masuda of Toppan Printing Co., Ltd., for his encouragement and support during the whole course of this study. The authors are also grateful to Eisaku Hayashi for his contribution in the construction of the acoustic micrometer. The ZnO transducers were made with a cooperation of colleagues at Tohoku University.

REFERENCES

- [1] H. H. Behncke, "Coating thickness measurement by the X-ray fluorescence method," *Metal Finishing*, vol. 82, no. 5, pp. 33-39, 1984.
- [2] M. Houze, B. Nongaillard, M. Gazalet, J. M. Rouvaen, and C. Bruneel, *J. Appl. Phys.*, vol. 55, pp. 194-198, 1984.
- [3] R. D. Weglein, "Acoustic microscopy applied to SAW dispersion and film thickness measurement," *IEEE Trans. Sonics Ultrason.*, vol. SU-27, no. 2, pp. 82-86, 1980.
- [4] J. Kushibiki and N. Chubachi, "Material characterization by line-focus-beam acoustic microscopy," *IEEE Trans. Sonics Ultrason.*, vol. SU-32, no. 2, pp. 189-212, 1985.
- [5] J. H. Bruning, D. R. Herriott, J. E. Gallagher, D. P. Rosenfeld, A. D. White, and D. J. Brangaccio, *Appl. Opt.*, vol. 13, pp. 2693-2703, 1974.
- [6] N. A. Massie, R. D. Nelson, and S. Holly, *Appl. Opt.*, vol. 18, pp. 1797-1803, 1979.
- [7] Y. Tsukahara, E. Takeuchi, E. Hayashi, and Y. Tani, "A new method

of measuring surface layer-thickness using dips in angular dependence of reflection coefficients," in *Proc. IEEE Ultrason. Symp.*, 1984, pp. 992-996.

- [8] E. Takeuchi, Y. Tsukahara, E. Hayashi, H. Masuda, and Y. Tani, "Application of reflection coefficient dip to layer thickness measurement by acoustic microscope," *Jpn. J. Appl. Phys.*, vol. 24, suppl. 24-1, pp. 190-192, 1985.
- [9] L. M. Brekhovskikh, *Waves in Layered Media*. New York: Academic Press, 1980, pp. 41-60.
- [10] K. Sezawa and K. Kanai, *Bull. Earthquake Res. Inst.*, vol. 13, pp. 237-244, 1935.
- [11] B. A. Auld, *Acoustic Fields and Waves in Solids*, vol. 2. New York: John Wiley, 1972, pp. 94-104.
- [12] D. E. Chimenti, A. H. Nayfeh, and D. L. Butler, "Leaky Rayleigh waves on a layered half space," *J. Appl. Phys.*, vol. 53, no. 1, pp. 170-176, 1982.
- [13] J. Kushibiki and N. Chubachi, "Application of LFB acoustic microscope to film thickness measurements," *Flectron. Lett.*, vol. 23, no. 12, pp. 652-654, 1987.
- [14] Commercial model used in this study was Dektak, manufactured by Sloan Technology Corporation.



Yusuke Tsukahara (M'85) was born in Chiba prefecture, Japan, on June 25, 1952. He received the B.S. degree in Physics from Waseda University, Tokyo, Japan, in 1976.

From 1976 to 1982 he was engaged in research and development of instruments for nondestructive testing at Ishikawajima Inspection Services Co. Ltd., Tokyo, Japan. Since 1982, he has been a researcher at Technical Research Institute of Toppan Printing Co. Ltd., Saitama, Japan, where he has been involved in the study of surface layers

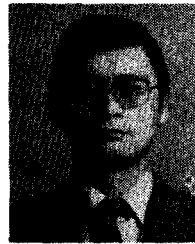
by ultrasonic spectroscopy. In 1986 he stayed at Tohoku University, Sendai, Japan, as a visiting researcher. His current interests include digital signal processing, image processing, speech analysis, ultrasonics and its application to the material evaluation.

He is a member of Acoustical Society of Japan.



Noritaka Nakaso was born in Tottori prefecture, Japan, in March 1960. He received the B.S. degree in Materials Science from Hiroshima University, Hiroshima, Japan, in 1985.

He has been employed at Technical Research Institute of Toppan Printing Co. Ltd., Saitama, Japan, since 1985. In 1987, he was involved in the application of scanning acoustic microscope (SAM) as a visiting researcher at Tohoku University, Sendai, Japan. His current interests include estimation of adhesion and application of SAM.



Jun-ichi Kushibiki (M'83) was born in Hirosaki, Japan, on November 23, 1947. He received the B.S., M.S., and Ph.D. degrees in electrical engineering from Tohoku University, Sendai, Japan, in 1971, 1973, and 1976, respectively.

In 1976 he became a Research Associate at the Research Institute of Electrical Communication, Tohoku University. Since 1988 he has been an Associate Professor at the Department of Electrical Engineering, Faculty of Engineering, Tohoku University. He has been studying ultrasonic metrology, especially acoustic microscopy and its applications, and recently established a method of material characterization by the line-focus-beam acoustic microscopy. He also has been interested in biological tissue characterization in the higher frequency range, applying both bulk and acoustic microscopy techniques.

Dr. Kushibiki is a member of the Institute of Electronics, Information and Communication Engineers of Japan, the Acoustical Society of Japan, and the Japan Society of Ultrasonic in Medicine.

Dr. Kushibiki is a member of the Institute of Electronics, Information and Communication Engineers of Japan, the Acoustical Society of Japan, and the Japan Society of Ultrasonic in Medicine.



Noriyoshi Chubachi (M'83) was born in Kokura, Japan, on October 5, 1933. He received the B.S., M.S., and Ph.D. degrees in electrical engineering from Tohoku University, Sendai, Japan, in 1956, 1962, and 1965, respectively.

In 1965 he joined the Research Institute of Electrical Communication, Tohoku University, where he was an Associate Professor from 1966 to 1978. Since 1979 he has been a Professor at the Department of Electrical Engineering, Tohoku University. From 1982 to 1983 he was a visiting

Professor of Electrical and Computer Engineering, University of California, Santa Barbara, CA. He has worked on ultrasonic transducers and delay lines, surface acoustic devices, acoustoelectronics, piezoelectric materials, acoustic microscopy, and related problems.

Dr. Chubachi is a member of the Institute of Electronics and Communication Engineers of Japan, the Society of Japanese Applied Physics, the Acoustical Society of Japan, the Japan Society of Ultrasonics in Medicine, and the Japan Society of Nondestructive Inspection. He served as chairman, Tokyo chapter of IEEE UFFC Society, from 1987 to 1988.